The HARC Holographic Imaging Facility - Multistatic Images of Distributed Targets

A.J. Blanchard, B. Williams, R.F. Schindel, B. Jersak, B. Krenek

Space Technology and Research Center Division of the Houston Advanced Research Center
800 Research Forest Dr. The Woodlands, TX USA 77381
Phone (713) 363-7922 FAX (713) 363-7923

ABSTRACT

The current literature has identified a number of theoretical approaches to microwave imaging technologies. The most common include ISAR and synthetic aperture radar. Both of these techniques use fixed relative positions between the transmitter and receiver (monostatic or quasi-monostatic in most cases). However, the generalized inverse imaging theory can accommodate more geometric configurations as well as frequency diversity. To date, there has been very little experimental evidence of microwave inverse imaging approaches which allow independent motion between transmitter and receiver. Recently, the Houston Advanced Research Center (HARC) developed an experimental measurement facility capable of such arrangements. This paper will present a description of the facility, its capability and some calibration results which are indicative of its performance. The ability to acquire images using unconventional geometries is investigated using mono-static and multi-static configurations. Very few measurements have been acquired from distributed targets using these unconventional techniques. We present measurements of a distributed scattering surface using discrete scattering elements (facet model representation) in the 18-26 GHz frequency range using three geometric configurations.

Key Words (Imaging, Inverse Problems, Synthetic Aperture Radar, Measurements, Distributed Targets)

INTRODUCTION

The use of RADAR derived images in earth/land and sea applications has been researched for several decades (Ulaby et.al., 1982). The development of synthetic aperture radar in the early 50's allowed high resolution images in the microwave spectrum to be recovered. The technologies associated with radar imaging have remained relatively constant. Applications have been developed and the hardware technologies improved, however, the basic premise for imaging has remained range doppler processing. The theoretical foundations of the range doppler imager (SAR) exists in generalized inversion theory. The implementation of SAR imagers in the form of a doppler and bandwidth processor is simply a matter of technology, not a requirement of the theory. There are a number of geometric implementation schemes that do not require doppler to obtain high resolution. These configurations can include mono-static, bistatic and multi-static geometries. To illustrate high resolution imaging without doppler processing, three data sets and angle processed images are presented.

The first two data sets presented were recovered using a fixed transmit-receive geometry (both bistatic and monostatic) with target rotation and frequency diversity. The third data set is a result of multistatic geometry and frequency diversity. Inversion algorithms reconstruct the phase locked linear polarized images. The implication in the comparison of these data sets is that different information bases are recovered when different geometric configurations are utilized. For mono-static and fixed bistatic configurations data can be interpreted as an equivalent radar cross section averaged over the angular aperture The multi-static configuration allows only one set of equivalent sources to be illuminated on the target. The recovered image can be interpreted as a set of equivalent sources rather than radar cross section. Additional investigation is required to determine which data base is more useful.

The theoretical basis for the imaging concept has its roots in the generalized inverse problem (Langenberg 1987, Farhat 1984, Devany 1983). The general problem is one of measuring complex field information and attempting to invert it to represent the physical parameters of the object causing the scatter. The relation between the object generated field and the source is given by the Porter-Bojarski equation.

Depending on the measurement configuration, signal processing of the measurements will produce either a 2-D projection image, or a full 3-D representation of the target (Devany 1983, Schindel 1989, Blanchard et.al. 1988). Several measurement configurations can be used. In the 2-D mode, the measurement surface can be formed using 2-D angular diversity, or 1-D angular diversity in conjunction with frequency diversity. Rotation is used to synthesize the aperture. In this measurement mode the scattering centers in the target are sampled in both frequency and angle and the integrated result of the RCS values are displayed at the appropriate location in the image.

The multi-static configuration involves the use of a fixed transmitter relative to the target, a rotating receiver, and frequency diversity (Schindel 1989). Receiver rotation measurement schemes combine monostatic and bistatic data. In addition, since only a single illumination direction is used, a single set of secondary sources is excited. This is not the case with object rotation measurement schemes, where the illumination direction is varied. From a data acquisition viewpoint, frequency diversity offers the most economical method of data acquisition and wide bandwidth significantly increases image resolution.

1. IMAGING FACILITY

Radar cross-section (RCS) measurements are obtained by recovering signals scattering from a target. The signals that reflect off the target typically scatter in all directions. Those signals that reflect straight back from the target are referred to as the monostatic return.

Several advantages in building a chamber to measure monostatic RCS are the ease and straight-forwardness of the design and the short lengths (less attenuation) of the semi-rigid cabling. However, a disadvantage is the fact that only the backscatter return is measured. For many targets, this is only a small percentage of the scattered response.

If the transmit and receive antennas are in two different locations, the measured response is known as the bistatic RCS. For a bistatic RCS chamber, the antennas can be placed in fixed locations or placed on moveable platforms. If the antennas are placed in fixed locations, several receive antennas would typically be needed to cover multiple angles as well as a switching network to select between them. On the positive side, semi-rigid cabling could be used, which with relatively lower loss than flexible coax, has good phase stability. If the antennas are placed on moveable platforms, only a single receive antenna would be needed along with a mechanism to move the antenna. However, expensive and relatively higher loss flexible cabling would be needed. Unlike the fixed antenna scenario, a moveable antenna could be placed anywhere (depending on the limitations of the movement mechanism) allowing data to be acquired which would be impractical in the fixed antenna scenario.

The necessity of recovering image information with three geometric configurations places special requirements on the design and construction of a measurement facility. The Space Technology and Research Center of the Houston Advanced Research Center, has constructed a bistatic RCS chamber with both the transmit and receive antennas placed on separate moveable platforms, with the ability to perform fully polarimetric measurements at arbitrary bistatic angles.

2. CHAMBER DESCRIPTION

The internal dimensions of the chamber are 30′ × 30′ × 30′ 6″ high. The main components of the chamber are sketched in Figure 1. These include the ground level maintenance access door, second floor target access door, fixed transmitter truss, transmitter trolley and antenna, moveable receiver truss, receiver trolley and receive antenna, azimuth positioner and support stand, and the target support pedestal. Some of these can be seen in Figure 2.

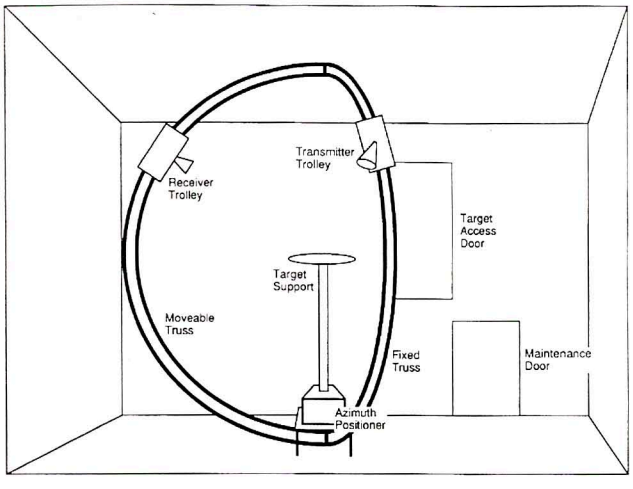

Fig. 1 - Sketch of the HARC/STAR holographic imaging facility showing the major components of the chamber.

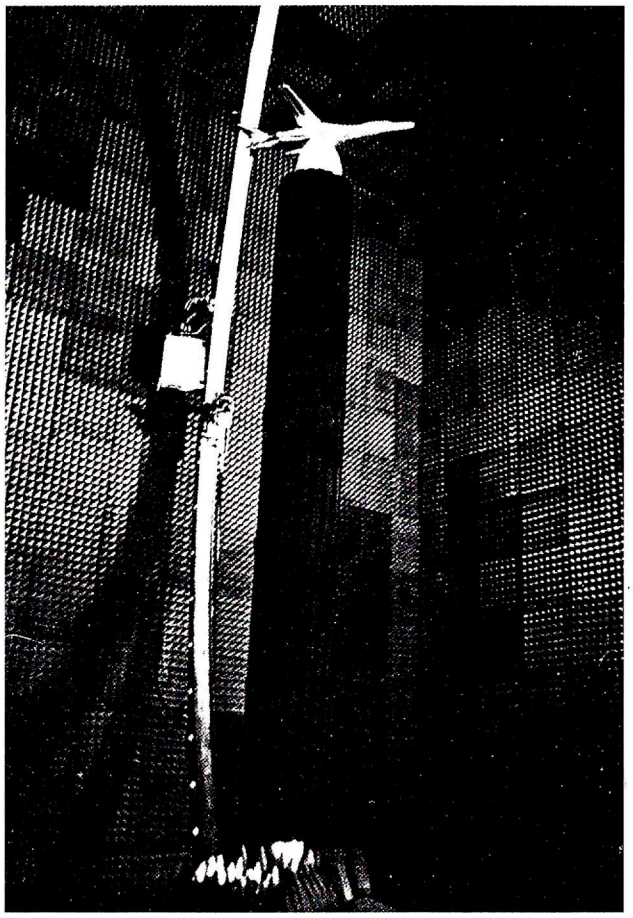

Fig. 2 - View of chamber showing receiver truss, trolley and azimuth positioner assembly.

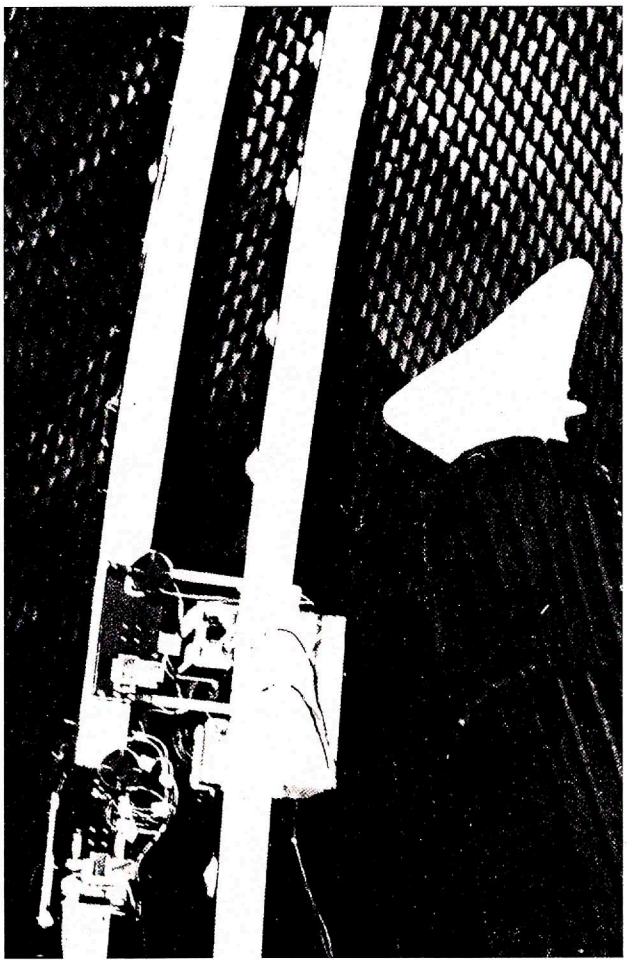

Fig. 3 - (Rotated 90 counter-clockwise) Detail view showing both the transmitter trolley (right) and the receiver trolley (left). Notice offset of transmitter antennas. The semi-rigid cables shown are

The trusses, which support the moveable transmit and receive trolleys, are identical except for their respective mountings. The transmitter truss is rigidly mounted at 0° azimuth while the receiver truss is mounted on spherical thrust bearings which allow motion about a vertical axis through a range of 0° to 180° in azimuth. The two trusses are made of aluminum and weigh approximately 1500 pounds each.

Each truss has an outside diameter of approximately 29 feet and inside diameter of 27 feet. Groves were machined at the four outside corners of each truss where the wheels of the trolleys ride. A 22 inch diameter gear is attached to the bottom of the moveable truss. A belt is attached to this gear which is in turn driven by a dc stepper motor. The stepper motor is computer controlled allowing for automated motion. The moveable truss can be placed parallel to the fixed truss for backscatter measurements.

The antennas and associated equipment are mounted on the transmitter and receiver trolleys. Both trolleys can be seen in Figure 3. The transmitter trolley contains the transmit antennas, the RF source, two amplifiers, a coupler, assorted switches and semi-rigid cabling. The fixed transmitter truss is parallel to but offset 16 inches from the 0m azimuth position. To compensate for this fact, the transmitter antenna face plate has been offset by the same 16 inches. Since the fixed transmitter truss is exactly parallel to the 0° azimuth position, the offset of the antenna face plate corrects for the offset of the transmitter truss. Thus, the transmit antennas always remain at a true 0° azimuth. The receiver trolley contains the receive antennas (which are identical to the transmit antennas), various mixers, assorted switches, and semi-rigid cabling.

Both the transmitter and the receiver trolleys are free to move along their respective trusses. If 0° elevation is defined as being directly above the target, both trolleys can move from 10°, where they contact the chamber ceiling, to approximately 165° in elevation.

Each trolley is attached to a belt which runs up the outside of its truss to the ceiling wrapping around an idler wheel inside the top of the truss, down the inside of the truss to

the ground around a drive wheel where it passes to the outside of the truss to the trolley. Computer driven dc stepper motors identical to the one used to move the receiver truss in azimuth are located at the base of each truss to control the elevation movement of the two trolleys. Both trolley and antennas remain at the same radial distance from the target throughout their range of motion.

The RF source is placed on the transmitter trolley near the transmit antennas to reduce loss associated with cable length. Mixers are placed on the receiver trolley to avoid having to run RF cables back to the receiver. By mixing at the receiver trolley low loss 20MHz IF is delivered over the long distance to the HP 8510 receiver.

The entire chamber is lined with 4 × 8 foot sheets of 24 gauge galvanized steel. This steel lining helps shield the chamber from outside RF energy. Additionally, the steel lining is grounded to a copper rod driven into the ground to prevent static electricity from building up in the chamber and possibly causing damage to equipment and/or personnel. Eight inch pyramidal absorber is used throughout the chamber. Although larger pyramidal absorber would have performed better at the lower frequencies, eight inch performs better at the higher frequencies of interest. A final problem with the absorber was the inability to optimize the absorber for minimum scattering and maximum absorption due to the fact that both the transmit and the receive antennas move. What is optimal for one transmit/receive orientation is seldom optimal for another, therefore, gating the received data is important for removal of spurious reflections.

Access to the target is accomplished by way of a platform which extends from the second floor. When extended this platform is about 12 feet above ground and lies next to the control room housing the computer and HP 8510 allowing for convenient access to the target during measurements. The other door to the chamber is on the ground floor designed for maintenance access only.

3. EQUIPMENT DESCRIPTION

The radar equipment is designed around the HP 8510 vector network analyzer. The system currently uses an HP 8510B, with an 8510C upgrade on order. Instead of an HP 8511 frequency converter, the system uses a distributed mixer system. The main RF source is an HP 83642A synthesized sweeper. The LO source is an HP 83622A synthesized sweeper and the test set is an HP 85309A LO/IF unit.

The system frequency span of 2-40 GHz is divided into three separate functional bands. These are 2-18 GHz (low band), 18-26.5 GHz (mid band), and 26.5-40 GHz (high band). Each of these bands makes use of a different set of antennas. The low band antennas are dual polarized, quad-ridged, conical horn antennas sold by the Dalmo Victor division of the General Instrument Corporation. Since these antennas are dual polarized, only a single transmit and receive antenna is needed. Standard waveguide fed rectangular horn antennas are used for mid and high band. Since each antenna produces a single polarization a transmit receive pair is used for each of the mid and high bands. The custom horn mountings can be seen in Figure 8 where only the low and mid band antennas are actually present. The low band makes use of an HP 8349B amplifier and fundamental mixing. Mid and high bands use an Avantek AWT-40058-22 amplifier with third harmonic and eighth harmonic mixing respectively. The different mixer systems are somewhat complex and will not be described here.

The computer used to automate the system is an HP series 9000 model 360 with 16 Mbytes of physical memory, 750 Mbytes of hard disk space, tape backup system, and ethernet/internet connection. The computer is running HP-UX, HP's version of UNIX. We are also using HP's Visual Engineering Environment (VEE) to develop all chamber control software. VEE is an iconic based development system with built in presentation graphics and graphical ability.

Azimuth position is set by a Scientific Atlanta 51050A controlled by a Scientific Atlanta 4131-3. The controller is programmable allowing automated target rotation.

4. MEASUREMENT CAPABILITIES

The chamber is capable of performing fully polarimetric measurements. Vertical polarization is defined in the theta unit vector direction, horizontal polarization in the phi unit vector direction. The four polarizations measurable are VV, HV, VH, and HH.

The ranges of motion for the transmit and receive antennas are as follows: (see Figure 4)

Transmit: $\Phi = 0°$, $10° \leq 0 \leq 165°$
Receive: $0° \leq \Phi \leq 10° \leq \theta \leq 165°$

Example output performance of the chamber is illustrated in Figures 5 and 6. These results represent a comparison between theoretical and measured values in the 2 to 18 GHz and 18 to 26 GHz frequency bands. Three representations of the measured results are shown including frequency, phase and time response to a 6 inch reference target. Several performance features are noteworthy. In the 2 to 4 GHz band the low frequency response of the chamber shows some coupling interference to support structures and lack of effectiveness of the absorber at low

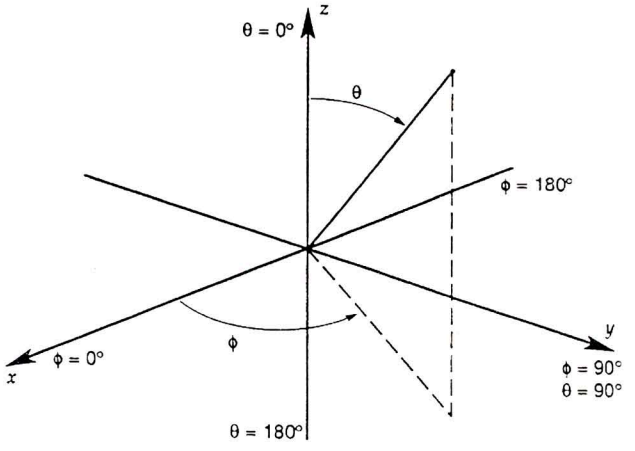

Fig. 4 - Angular definitions and measurement system geometry.

frequencies. Phase linearity suffers in the same region, however, phase performance of the RF system is exceptionally good through the entire 4 to 26 GHz frequency band. The time domain plot of Figure 5(c) shows the return from the sphere and creeping wave. Both bands display a noise floor below -90 dBsm. Note the fuzziness of Figure 6(a) is due to the fine resolution of the magnitude scale with 0.05dB increments.

4.1 Distributed Target Measurement Experiment

The target used for the distributed clutter measurements is shown in Figure 7. The target consists of a set of specular scatterers, in this case 2 inch diameter metallic disks. These scattering elements are distributed in both azimuth and elevation angle in a predetermined random pattern. The azimuth angle distribution is uniform while the elevation angles are normally distributed. Each of the scattering elements are mounted on a polyurethane core, shown in Figure 8, to maintain the required preset angles. The entire structure is glued to a 5 foot diameter mounting base. Approximately 200 scattering elements were used.

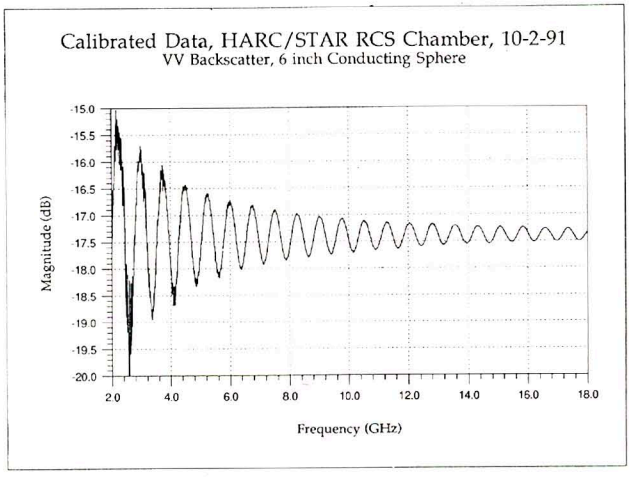

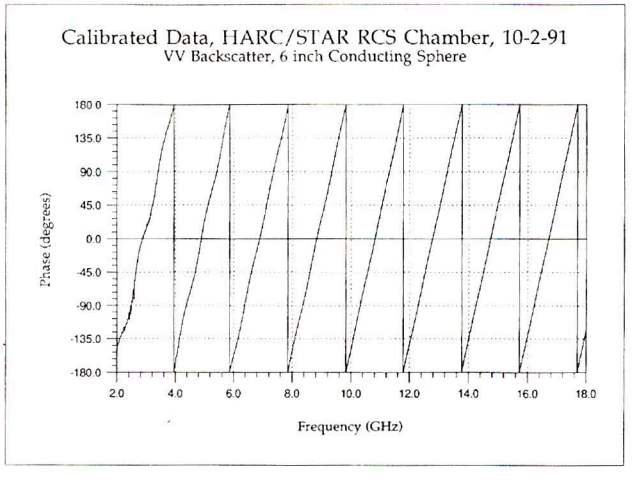

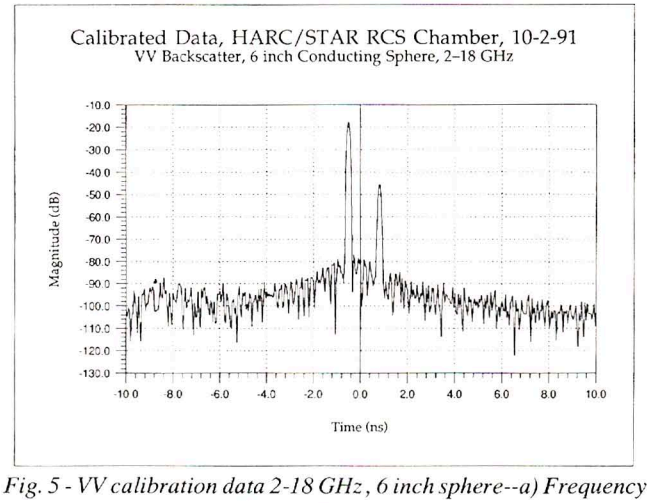

Fig. 5 - VV calibration data 2-18 GHz, 6 inch sphere--a) Frequency response, b) Phase response, c) Time domain response.

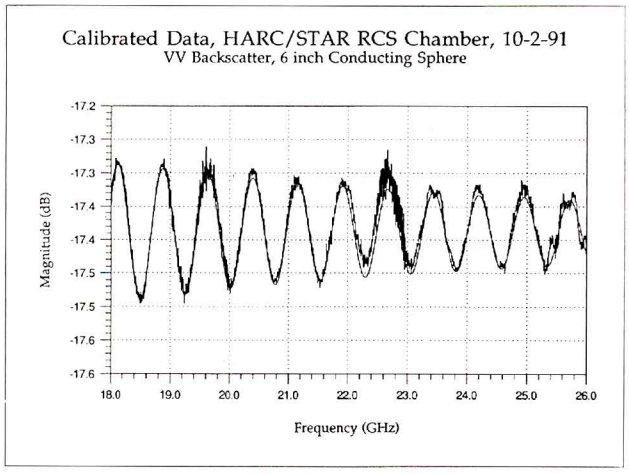

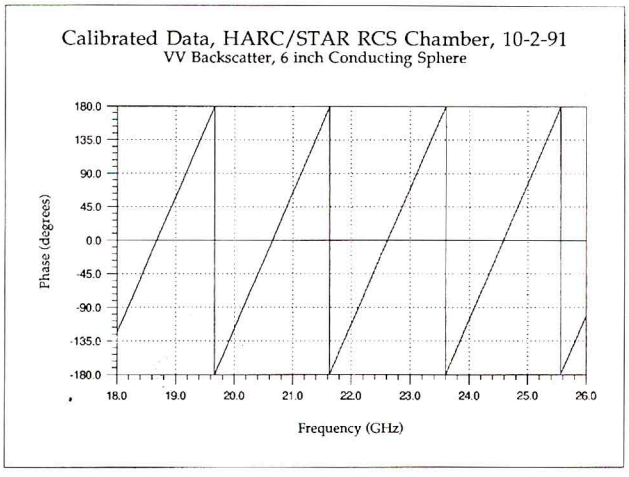

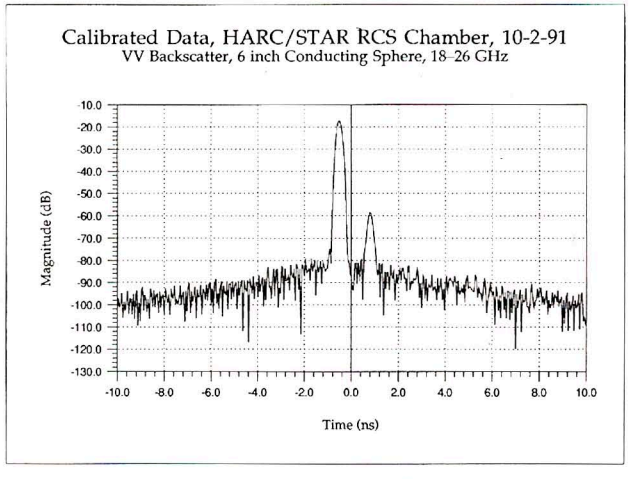

Fig. 6 - VV calibration data 18-26 GHz , 6 inch sphere--a) Frequency response, b) Phase response, c) Time domain response.

Monostatic image data was acquired over a frequency range extending from 18 to 26 GHz with the receiver and transmitter elevation at approximately 45 degrees. The quasi-monostatic arrangement places the receiver at about 1.7 degrees in azimuth from the transmitter which is at zero azimuth. There were 101 frequency samples between the two frequency boundaries and the positioning table was rotated from 0-360 degrees in 0.5 degree steps. All four polarizations were sampled. Calibration data sets were taken for the 6 inch sphere and it's associated support.

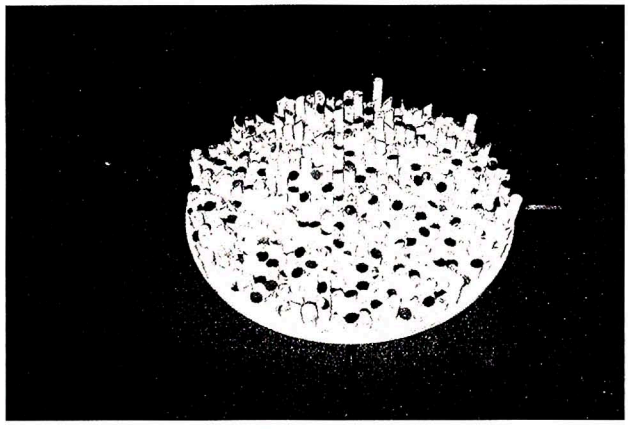

Fig. 7 - Target structure with individual scattering elements.

Fig. 8 - Detail of the support structures for each specular element.

All low band measurements were taken first. A bistatic angle of 45 degrees with all other parameters as noted above was then acquired. Finally a multistatic set with azimuth increments of 0.5 degree was made from 7 to 180 degrees for a 173 degree aperture.

frequency	18-26.5GHz
points	101 used
Tx el	45deg
Rx el	45
Tx az	0
Rx az mono	1.7
Rx az bi	45
Rx az multi	7-180
Rx az steps multi	0.5deg
pols	vv,vh,hv,hh

7. MEASUREMENT ANALYSIS

The measured results are described in this section. This target, represents a distribution of specular scattering cent-

ers. Only a limited number of scatterers were included in this experiment in order to obtain the proper statistical distribution. The microwave data taken in the 18 to 26 GHz band should represent quasi-optical information. In an effort to experimentally identify which scatterers might have been illuminated, several optical measurements were made. Photographs were taken under varying azimuth illumination directions, with a constant elevation angle of 45 degrees for both light source and camera to simulate the microwave imaging experiment parameters. Figure 9 represents the monostatic measurements configuration with the light source and the camera at the 0 degree azimuth position. Figure 10 represents the bistatic geometry with the illuminator at the 0 degree azimuth position and the camera at the 45 degree azimuth position. Several points are evident from this optical experiment. Only a very few scatterers are visible at any particular azimuthal position. Certain scattering elements near the 45° elevation angle are visible. A different set of scatterers become illuminated at different azimuth angles. The bistatic configuration will select a prescribed set of scattering centers given by the angle between the illuminator and detector. Finally, for both cases the specular scattering centers selected are very well defined by the geometry of the experiment.

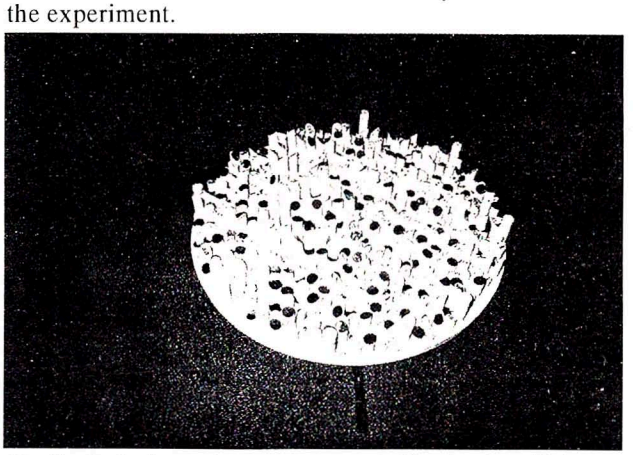

Fig. 9 - Optical experiment --monostatic illumination, 45 degrees incident angle.

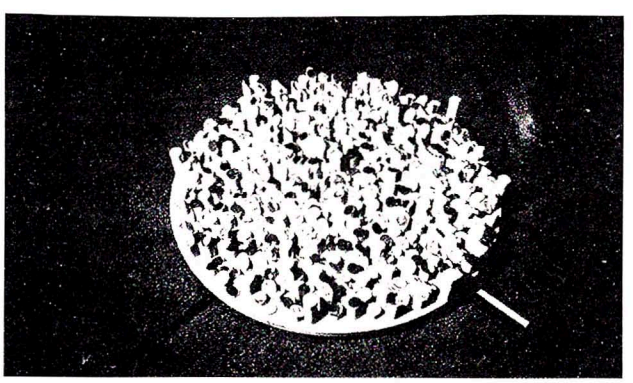

Fig. 10 - Optical experiment --bistatic illumination, 45 degrees incident angle, 0 degrees azimuth illumination, 45 degrees azimuth receiver.

While the geometric conditions for the microwave measurements are the same as the optical measurements, there are significant differences in the imaging processes. The optical images are recovered by a real aperture system with enough gain to produce the resolution shown in the previous photographs. The microwave system uses a synthesized aperture to produce high resolution. This angular aperture is significantly larger (180 to 360 degrees in the case of these measurements) than the optical one.

The microwave images are illustrated in Figures 11, 12, and 13. Each figure represents the image data in two formats, spectral information at the top (frequency response with azimuth angle) and spatial information at the bottom (image). Both the bistatic and monostatic spectra show a distribution of scattering intensity as a function of azimuth angle. The frequency response of the target is relatively constant, as demonstrated by comparing individual rings. However, there are certain angular regions where very little scattering information exists. This is to be expected since there will be angular positions where specular scatterers will not be illuminated.

It is interesting to note that the same scatterers are illuminated in both the monostatic measurements and bistatic measurements. In addition the inversion algorithm automatically accounts for the rotational differences that occur between mono and bistatic geometries. The two images are almost identical.

There is a great deal of difference between the target rotation images shown in Figures 11 and 12 and the multi-static image generated by receiver rotation of Figure 13. In the latter case the illuminated sources are constant (transmitter is fixed at 0° azimuth and 45° elevation) and the receiver maps the far field radiated structure of the scatterers. The image identifies a greater number of scattering sources and the dynamic range is significantly greater. The final conclusion indicates that there is significantly different information recovered using multistatic geometries compared to mono and bistatic geometries.

REFERENCES

A. J. Blanchard, M. Dolaty, "Bistatic Frequency Diverse Imaging of Complex Scattering Targets", Proceedings of IGARSS '88 Symposium, Edinburgh, Scotland, 13-16 Sept., 1988.

A. J. Devaney, "A Filtered Backpropagation Algorithm for Diffraction Tomography", IEEE Transactions on Biomedical Engineering, Vol. BME-30, no. 7, July 1983.

N. H. Farhat, C. L. Werner, T. H. Chu, "Prospects for Three-Dimensional Projective and Tomographic Imaging Radar Networks", Radio Science, Vol. 19, pp. 1347-1355, Sept.-Oct. 1984.

K. J. Langenberg: "Applied Inverse Problems for Acoustic, Electromagnetic, and Elastic Wave Scattering" in: Basic Methods of Tomography and Inverse Problems. Ed.: P.C. Sabatier, Adam Hilger, Bristol 1987.

Schindel, R. F., Experimental Diverse Microwave Holography, PhD Dissertation, University of Texas at Arlington, Arlington, Texas, December 1989.

F.T. Ulaby, R.K. Moore, A.K. Fung, Microwave Remote Sensing: Active Passive, Vol. II, Dedham, Ma., Artech House, 1982.

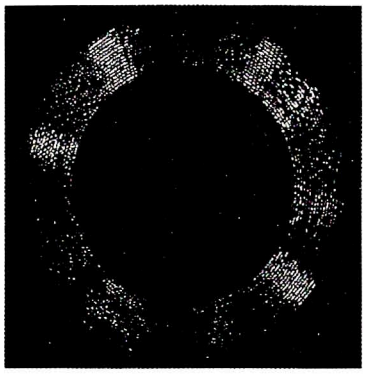

Fig. 11 - Microwave imaging results monostatic measurements a) spectral plot, b) Image output.

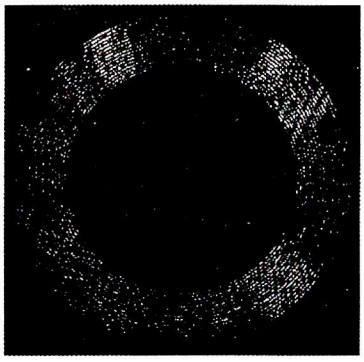

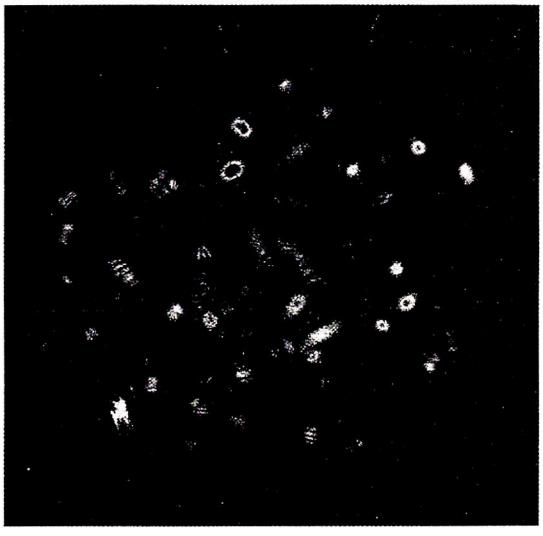

Fig. 12 - Microwave imaging results bistatic measurements a) spectral plot, b) Image output.

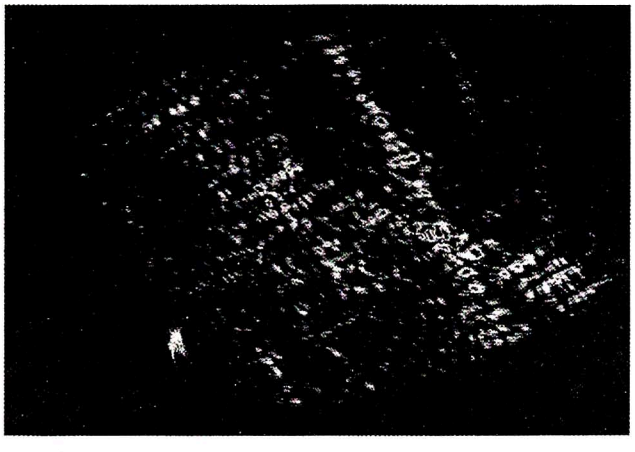

Fig. 13 - Microwave imaging results multistatic measurements a) spectral plot, b) Image output.